

# Randomized Kaczmarz for Tensor Linear Systems

Anna Ma and Denali Molitor

January 14, 2022

## Abstract

Solving linear systems of equations is a fundamental problem in mathematics. When the linear system is so large that it cannot be loaded into memory at once, iterative methods such as the randomized Kaczmarz method excel. Here, we extend the randomized Kaczmarz method to solve multi-linear (tensor) systems under the tensor-tensor t-product. We provide convergence guarantees for the proposed tensor randomized Kaczmarz that are analogous to those of the randomized Kaczmarz method for matrix linear systems. We demonstrate experimentally that the tensor randomized Kaczmarz method converges faster than traditional randomized Kaczmarz applied to a naively matricized version of the linear system. In addition, we draw connections between the proposed algorithm and a previously known extension of the randomized Kaczmarz algorithm for matrix linear systems.

## 1 Introduction

Methods for processing and analyzing large datasets have seen rapid development and use in signal processing and machine learning. For example, in the machine learning community, recommender systems and collaborative filtering have become ubiquitous tools for understanding user behavior and preferences. Data is commonly interpreted in this setting as a user-item matrix. As another example, consider the process of recovering a compressed video. Videos are understood to be a collection of image frames and images are often vectorized so that the signal associated with a video is a pixel location by frame matrix.

One reason data are often organized in this two dimensional (user-item, pixel-frame, etc.) fashion is because a vast majority of the existing methods operate on data that are stored as matrices and vectors. Recommender systems employ matrix factorization [18]. Sparse optimization and multiple measurement vector methods are common approaches for video recovery [22, 20]. In such approaches, optimization frameworks expect data in the form of one or two dimensional arrays (i.e., vectors and matrices). However, in reality, data can be higher multidimensional arrays and this restriction to the one or two dimensional representations often destroys structure (for example, spatial or

temporal structure) inherent to the data. In video recovery, data occurs naturally as a third-order tensor with dimensions image width by image height by frame number. Commonly, images are vectorized to form columns of the pixel by frame data matrix, which destroys the spatial correlation within the frames.

In the seminal paper of [17], the authors define a closed multiplication operation between two tensors referred to as the *t-product*. Initially motivated for tensor factorization, use of the t-product has become prominent in the tensor and signal processing community. Under the t-product, tensors enjoy a linear algebraic-like framework that has proved useful in applications such as dictionary learning [33, 38], low-rank tensor completion [41, 32, 39, 40], facial recognition [11], and neural networks [27, 36]. The process of *naively* transforming high-order tensors into two dimensional arrays via a flattening or unfolding process is often referred to as “matricization”. Since the t-product acts as a linear operator directly on higher-order tensors, it avoids matricization and preserves multidimensional structure.

Here, we consider the fundamental problem of solving large linear systems of equations for third-order tensors under the t-product. In the matrix linear system setting, randomized iterative methods are a popular choice for solving or finding approximate solutions to systems that are too large to load into memory at once [7, 21, 34].

One such randomized iterative method is the known as the randomized Kaczmarz method. The randomized Kaczmarz method (MRK)<sup>1</sup> is closely related to other popular randomized iterative methods such as stochastic gradient descent and coordinate descent and is commonly used in computed tomography (CT imaging) and other signal processing applications [26, 9].

In this work, we propose a Kaczmarz-type iterative methods for tensor linear systems under the t-product which we refer to as tensor randomized Kaczmarz (TRK). We analyze the convergence of TRK and derive theoretical guarantees for the proposed method in two variations. The first approach analyzes TRK from a similar lens as MRK, i.e., views iterates as projections onto solution spaces of a subsampled system. The second approach takes advantage of the fact that the t-product can be efficiently computed in Fourier space. In addition to proving theoretical guarantees for TRK, we also make connections between TRK and other variants of MRK. Our theoretical findings are supported by numerical experiments before we conclude our work with final remarks. We view this analysis as a case study with a template to extend other methods to the tensor setting under the t-product.

## 1.1 Randomized Kaczmarz

Randomized Kaczmarz is an iterative method for approximating solutions to linear systems of equations [13]. The MRK method uses iterative projections

---

<sup>1</sup>While the randomized Kaczmarz literature typically abbreviates randomized Kaczmarz as RK, throughout this work, MRK is used to distinguish the matrix and tensor versions of randomized Kaczmarz.

onto the solution space with respect to a selected row to approximate the solution of a linear system. More specifically, for a linear system  $\mathbf{A}x = b$ , a row index  $i$  is chosen at each iteration of MRK and the current iterate (approximate solution) is projected onto the solution space

$$\mathbf{A}_{i:}x = b_i.$$

The method is advantageous for very large linear systems that cannot be loaded into memory at once. There are many extensions to MRK including greedy [1, 23, 10, 6, 29, 30, 4] and block [25] variants to speed convergence and an extended version for inconsistent linear systems [24, 42]. The MRK method and its block variant fall under the more general sketch-and-project framework which additionally includes other popular methods such as coordinate descent [9]. Strohmer and Vershynin demonstrated that MRK converges exponentially in expectation when indices  $i$  are sampled with probabilities proportional to the squared row norms  $\|\mathbf{A}_{i:}\|^2$  [34]. When the rows of  $\mathbf{A}$  are normalized, this is equivalent to sampling the indices uniformly at random. The standard MRK update for a linear system  $\mathbf{A}x = b$  is given by

$$x^{t+1} = x^t - \mathbf{A}_{i_t:}^* \frac{\langle \mathbf{A}_{i_t:}, x^t \rangle - b_{i_t}}{\|\mathbf{A}_{i_t:}\|^2}, \quad (1)$$

where  $i_t$  is the row index selected at iteration  $t$  and  $\mathbf{A}_{i_t:}^*$  is the transpose of the  $i_t^{\text{th}}$  row of  $\mathbf{A}$ . At each iteration  $t$ , the current iterate  $x^t$  is projected onto the solution space with respect to the row  $\mathbf{A}_{i_t:}$  of the measurement matrix  $\mathbf{A}$ .

For linear systems of the form  $\mathbf{A}\mathbf{X} = \mathbf{B}$  with  $\mathbf{X}$  and  $\mathbf{B}$  representing matrices, we can apply the MRK update of Equation (1) to each column of  $\mathbf{B}$  in order to recover each column of the signal  $\mathbf{X}$ . We can equivalently rewrite the MRK update for this case as

$$\mathbf{X}^{t+1} = \mathbf{X}^t - \mathbf{A}_{i_t:}^* \frac{\mathbf{A}_{i_t:}\mathbf{X}^t - \mathbf{B}_{i_t:}}{\|\mathbf{A}_{i_t:}\|^2}. \quad (2)$$

## 1.2 Tensor linear systems

Tensors arise in many applications and working with tensors directly, as opposed to naively flattening tensors into matrices can preserve significant structures and have computational advantages. Unfortunately, when working with tensors, many basic and fundamental linear algebraic constructs and results do not generalize naturally. For example, it is not obvious how one should define multiplication between two tensors [17, 3, 15, 5].

We specifically consider tensor linear systems under the tensor t-product. The t-product, proposed by Kilmer and Martin [17], is a bilinear operation between tensors, that allows for the generalization of many matrix algebra definitions and properties to the tensor setting. In particular, the t-product generalizes the concept of orthogonality between tensors, which is key for analysis of TRK. We provide further details about the t-product in Section 2.2.

A tensor linear system under the t-product is formulated as follows. Let  $\mathcal{X} \in \mathbb{C}^{\ell \times p \times n}$  be an unknown third-order tensor representing a three-dimensional data array. For example, this three-dimensional data could represent a video, color image, temporal data, or three-dimensional density values. A tensor linear system under the t-product is written as:

$$\mathcal{A}\mathcal{X} = \mathcal{B}, \quad (3)$$

with  $\mathcal{A} \in \mathbb{C}^{m \times \ell \times n}$ ,  $\mathcal{X} \in \mathbb{C}^{\ell \times p \times n}$  and  $\mathcal{B} \in \mathbb{C}^{m \times p \times n}$ .

Tensor linear systems arise in many applications. For example, factorization methods and dictionary learning have been extended to the tensor setting [43, 37, 35, 31, 2] and specifically with use of the t-product [17, 28, 33]. In practice, factorization methods such as non-negative matrix factorization depend on solving (potentially very large) linear systems as subroutines. As another example, consider extreme learning machines (ELM). Extreme learning machines are feedforward neural networks in which random weights are assigned for the hidden nodes [12]. A linear mapping of the hidden-layer outputs is then learned using a labeled set of training data. A major advantage of ELM is that learning the linear mapping of the hidden-layer outputs to the output layer is relatively simple and is independent of the activation functions used. Newman et al. proposed a tensor neural network intended for tensor data [27]. Their proposed networks use tensor-tensor products and enable the use of more compact parameter spaces [28]. Extending ELM to the tensor neural network setting leads to the need to solve (again potentially very large) tensor linear systems.

Randomized Kaczmarz is closely related to the popular optimization technique, stochastic gradient descent (SGD) [26]. Most related to this work is the tensor stochastic gradient descent that was recently implemented to train tensor neural networks under the t-product [27]. The focus of the aforementioned work is a tensor neural network framework for multidimensional data and does not delve into an algorithmic analysis of SGD under the t-product.

In this work, we introduce a Kaczmarz inspired iterative method that considers row slices of the tensor system at each iteration and provide theoretical analysis for the proposed method. To the best of our knowledge, no other works have consider solving large-scale linear t-product tensor systems with stochastic iterative methods.

### 1.3 Contributions

We propose TRK, a randomized Kaczmarz method for solving linear systems of third-order tensors under the t-product. We analyze the convergence of the proposed method and demonstrate its performance empirically. In the convergence analysis, we discuss projections and spectral constants for tensors under the t-product. We compare the performance of the proposed TRK method with a naively matricized MRK applied to a flattened tensor system. We also demonstrate that TRK is equivalent to performing block MRK [8] in the Fourier domain. This work serves as an example for extending methods for tensors un-

der the t-product and how the properties of the t-product in the Fourier domain can be used to analyze convergence in this setting.

## 2 Background and notation

In this section, we present notation and several linear algebraic results for tensors under the t-product.

### 2.1 Notation

Throughout, calligraphic capital letters represent tensors, bold capital letters represent matrices, and lower case letters represent vectors and scalars. The index  $i$  is reserved for indexing row slices of tensors (see Figure 1a), rows of matrices, and entries of vectors. The index  $j$  is similarly reserved for indexing column slices of tensors and columns of matrices. The index  $k$  is reserved for indexing frontal slices of tensors as illustrated in Figure 1b.

For matrices  $\mathbf{M}$ , we use the notation  $\mathbf{M}_{i:}$  and  $\mathbf{M}_{:,j}$  to represent the  $i^{\text{th}}$  row and  $j^{\text{th}}$  column respectively. We use  $\mathcal{M}_{i:}$  to represent row slices and  $\mathcal{M}_{::k}$  to represent frontal slices of a third-order tensor  $\mathcal{M}$  as shown in Figure 1. Because frontal slices of tensors are heavily used throughout this work, to condense notation, bold subscripted capital letters,  $\mathbf{M}_k$ , represents the  $k^{\text{th}}$  frontal slice of  $\mathcal{M}$  equivalently given by  $\mathcal{M}_{::k}$ , unless otherwise stated (for example, the  $n \times n$  DFT matrix  $\mathbf{F}_n$  and  $n \times n$  identity matrix  $\mathbf{I}_n$ ).

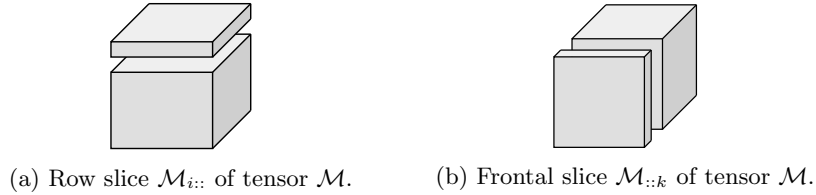


Figure 1: Row slice  $\mathcal{M}_{i:}$  and frontal slice  $\mathcal{M}_{::k}$  of tensor  $\mathcal{M}$ .

The squared Frobenius norm  $\|\cdot\|_F^2$  for matrices and tensors denotes the sum of squares of all scalar elements. For a matrix  $\mathbf{M}$ ,  $\|\mathbf{M}\|_F^2 = \sum_{ij} \mathbf{M}_{ij}^2$  and for a third-order tensor  $\mathcal{M}$ ,  $\|\mathcal{M}\|_F^2 = \sum_{ijk} \mathcal{M}_{ijk}^2$ . We use  $\sigma_{\min}(\mathbf{M})$  to denote the smallest singular value and  $\mathbf{M}^\dagger$  to denote the pseudoinverse of the matrix  $\mathbf{M}$ .

Equation (4) shows how a third-order tensor  $\mathcal{M}$  is unfolded into a matrix:

$$\text{unfold}(\mathcal{M}) = \begin{pmatrix} \mathcal{M}_{::0} \\ \vdots \\ \mathcal{M}_{::n-1} \end{pmatrix} = \begin{pmatrix} \mathbf{M}_0 \\ \vdots \\ \mathbf{M}_{n-1} \end{pmatrix}. \quad (4)$$

To revert the unfolding of a tensor  $\mathcal{M}$  we can fold the matrix in Equation (4) such that  $\text{fold}(\text{unfold}(\mathcal{M})) = \mathcal{M}$ . To condense notation, when using both

indices and transposes, the transpose are applied to the tensor or matrix slice, that is  $\mathbf{M}_{i:}^* = (\mathbf{M}_{i:})^*$  and  $\mathcal{M}_{i::}^* = (\mathcal{M}_{i::})^*$ .

The tensor product of tensors  $\mathcal{A}$  and  $\mathcal{B}$  is written as  $\mathcal{AB}$ . Similarly, for matrices  $\mathbf{A}, \mathbf{B}$ , their matrix product is written as  $\mathbf{AB}$ . We do not consider the products between tensors and matrices. Throughout, we use  $\mathcal{A}$  and  $\mathbf{A}$  to represent the measurement tensor and matrix,  $\mathcal{X}$ ,  $\mathbf{X}$ , and  $x$  to represent signal tensor, matrix and vector and  $\mathcal{B}$ ,  $\mathbf{B}$ , and  $b$  to represent the observed measurements for the linear systems

$$\mathcal{AX} = \mathcal{B}, \quad \mathbf{AX} = \mathbf{B}, \text{ and } \mathbf{Ax} = b.$$

Lastly, the index  $t$  is reserved only to indicate iteration number and the shorthand  $i \in [m-1]$  denotes  $i = \{0, 1, 2, \dots, m-1\}$ .

## 2.2 Tensor linear algebra

We now provide background on the tensor-tensor t-product[17]. Under the t-product one, can recover many standard linear algebraic properties such as transposes, orthogonality, inverses and projections.

The t-product is defined in terms of block-circulant matrices.

**Definition 1.** For  $\mathcal{A} \in \mathbb{C}^{m \times \ell \times n}$ , let  $\text{bcirc}(\mathcal{A})$  denote the block-circulant matrix

$$\text{bcirc}(\mathcal{A}) = \begin{pmatrix} \mathbf{A}_0 & \mathbf{A}_{n-1} & \mathbf{A}_{n-2} & \dots & \mathbf{A}_1 \\ \mathbf{A}_1 & \mathbf{A}_0 & \mathbf{A}_{n-1} & \dots & \mathbf{A}_2 \\ \vdots & \vdots & \vdots & \ddots & \vdots \\ \mathbf{A}_{n-1} & \mathbf{A}_{n-2} & \mathbf{A}_{n-3} & \dots & \mathbf{A}_0 \end{pmatrix} \in \mathbb{C}^{mn \times \ell n}. \quad (5)$$

The following definitions of tensor-tensor product, identity tensor, transpose, inverse, and orthogonality under the t-product are taken from Kilmer and Martin [17]. While the definitions and results here are specific to the t-product, this product has been generalized to a class of tensor products that use arbitrary invertible linear operators [14].

**Definition 2.** The tensor-tensor t-product is defined as

$$\mathcal{AB} = \text{fold}(\text{bcirc}(\mathcal{A}) \text{unfold}(\mathcal{B})) \in \mathbb{C}^{m \times p \times n},$$

where  $\mathcal{A} \in \mathbb{C}^{m \times \ell \times n}$  and  $\mathcal{B} \in \mathbb{C}^{\ell \times p \times n}$ .

**Definition 3.** The  $m \times m \times n$  identity tensor, denoted  $\mathcal{I}$ , is the tensor whose first frontal slice is the  $m \times m$  identity matrix and whose remaining entries are all zeros.

The identity tensor satisfies

$$\mathcal{MI} = \mathcal{IM} = \mathcal{M}$$

for all tensors  $\mathcal{M}$  with compatible sizes.

**Definition 4.** The conjugate transpose of a tensor  $\mathcal{M} \in \mathbb{C}^{m \times \ell \times n}$  is denoted  $\mathcal{M}^*$  and is produced by taking the conjugate transpose of all frontal slices and reversing the order of the frontal slices  $1, \dots, n-1$ .

Note that this definition ensures  $(\mathcal{M}^*)^* = \mathcal{M}$  and  $(\mathcal{AB})^* = \mathcal{B}^* \mathcal{A}^*$ . A tensor is symmetric if  $\mathcal{M}^* = \mathcal{M}$ .

**Definition 5.** A tensor  $\mathcal{M}$  is invertible if there exists an inverse tensor  $\mathcal{M}^{-1}$  such that

$$\mathcal{M}\mathcal{M}^{-1} = \mathcal{M}^{-1}\mathcal{M} = \mathcal{I}.$$

Note that for an invertible tensor  $\mathcal{M}$ ,

$$\mathcal{M}^* (\mathcal{M}^{-1})^* = \mathcal{M}^{-1} \mathcal{M} = \mathcal{I}$$

and

$$(\mathcal{M}^{-1})^* \mathcal{M}^* = \mathcal{M} \mathcal{M}^{-1} = \mathcal{I}.$$

Thus, we have  $(\mathcal{M}^*)^{-1} = (\mathcal{M}^{-1})^*$ .

**Definition 6.** A tensor  $\mathcal{Q} \in \mathbb{C}^{m \times p \times n}$  is orthogonal if

$$\mathcal{Q}^* \mathcal{Q} = \mathcal{I} = \mathcal{Q} \mathcal{Q}^*.$$

The following properties of block circulant matrices will be useful throughout. Proofs can be found in Appendix A.

**Fact 1.** For tensors  $\mathcal{A}$  and  $\mathcal{B}$ , the following equality holds:

$$\text{bcirc}(\mathcal{AB}) = \text{bcirc}(\mathcal{A}) \text{bcirc}(\mathcal{B}).$$

**Fact 2.** The block circulant operator  $\text{bcirc}(\cdot)$  commutes with the conjugate transpose,

$$\text{bcirc}(\mathcal{M}^*) = \text{bcirc}(\mathcal{M})^*.$$

### 2.2.1 Orthogonal tensor projections

These definitions and facts allow us to characterize orthogonal tensor projections under the t-product, which is key for proving convergence of TRK.

**Lemma 3.** If  $\mathcal{M}^* \mathcal{M}$  is invertible, then the tensor  $\mathcal{P} = \mathcal{M} (\mathcal{M}^* \mathcal{M})^{-1} \mathcal{M}^*$  is an orthogonal projection tensor.<sup>2</sup>

*Proof.* First, we show that  $\mathcal{P} = \mathcal{M} (\mathcal{M}^* \mathcal{M})^{-1} \mathcal{M}^*$  is a projection tensor, which follows by the following computation:

$$\begin{aligned} \mathcal{P}\mathcal{P} &= \mathcal{M} (\mathcal{M}^* \mathcal{M})^{-1} \mathcal{M}^* \mathcal{M} (\mathcal{M}^* \mathcal{M})^{-1} \mathcal{M}^* \\ &= \mathcal{M} (\mathcal{M}^* \mathcal{M})^{-1} \mathcal{M}^* \\ &= \mathcal{P}. \end{aligned}$$

---

<sup>2</sup>This result is also stated and discussed in [16]. We provide a proof here for completeness.

From the multiplication reversal property of the Hermitian transpose given in Proposition 4.3 of [14],

$$\begin{aligned}\mathcal{P}^* &= \left( \mathcal{M} (\mathcal{M}^* \mathcal{M})^{-1} \mathcal{M}^* \right)^* \\ &= \mathcal{M} \left( (\mathcal{M}^* \mathcal{M})^{-1} \right)^* \mathcal{M}^* \\ &= \mathcal{M} (\mathcal{M}^* \mathcal{M})^{-1} \mathcal{M}^* \\ &= \mathcal{P}\end{aligned}$$

and the tensor  $\mathcal{P}$  is an orthogonal projection.  $\square$

The convergence analysis of TRK, uses the following result.

**Lemma 4.** *If the tensor  $\mathcal{P} \in \mathbb{C}^{m \times m \times n}$  is an orthogonal projection,  $\text{bcirc}(\mathcal{P})$  is also an orthogonal projection.*

*Proof.* Since  $\mathcal{P}$  is symmetric,

$$\text{bcirc}(\mathcal{P})^* \stackrel{\text{Fact 2}}{=} \text{bcirc}(\mathcal{P}^*) = \text{bcirc}(\mathcal{P}).$$

To see that  $\text{bcirc}(\mathcal{P})$  is a projection, note that since  $\mathcal{P}$  is a projection tensor,

$$\text{bcirc}(\mathcal{P}) = \text{bcirc}(\mathcal{P}\mathcal{P}) \stackrel{\text{Fact 1}}{=} \text{bcirc}(\mathcal{P}) \text{bcirc}(\mathcal{P}).$$

$\square$

### 3 Tensor randomized Kaczmarz

Tensor randomized Kaczmarz is a Kaczmarz-type iterative method designed for t-product tensor linear systems. One notable difference between the t-product tensor and matrix linear systems is the interaction of the measurements  $\mathcal{A}_{i::}$  and  $\mathbf{A}_{i:}$  with the signals  $\mathcal{X}$  and  $x$ . For the products  $\mathbf{A}_{i:}x = b_i$  and  $\mathbf{A}_{i:}\mathbf{X} = \mathbf{B}_{i:}$ , each value in the signal  $\mathbf{X}$  or  $x$  is multiplied by a single element of the measurement  $\mathbf{A}_{i:}$ . In the tensor measurement product,

$$\mathcal{A}_{i::}\mathcal{X} = \text{fold}(\text{bcirc}(\mathcal{A}_{i::}) \text{unfold}(\mathcal{X})) \in \mathbb{C}^{n \times p}.$$

Since  $\text{bcirc}(\mathcal{A}_{i::}) \in \mathbb{C}^{n \times \ell n}$ , each element of  $\mathcal{X}$  is multiplied by  $n$  elements in  $\mathcal{A}_{i::}$  and affects  $n$  entries of the resulting product  $\mathcal{B}_{i::}$ . Equivalently, each frontal face of  $\mathcal{X}$  is multiplied by each frontal face of  $\mathcal{A}_{i::}$ . See Kilmer and Martin [17] for more details and intuition for the t-product.

We propose the following TRK update for tensor linear systems

$$\mathcal{X}^{t+1} = \mathcal{X}^t - \mathcal{A}_{i_t::}^* \left( \mathcal{A}_{i_t::} \mathcal{A}_{i_t::}^* \right)^{-1} \left( \mathcal{A}_{i_t::} \mathcal{X}^t - \mathcal{B}_{i_t::} \right). \quad (6)$$

The  $\mathcal{A}_{i::}$  are row slices of the tensor  $\mathcal{A}$  as depicted in Figure 1a. The index  $i_t$  used at each iteration is selected according to a probability distribution over the row indices  $i \in [m-1]$ . The TRK algorithm is detailed in Algorithm 1.



---

**Algorithm 1** Tensor RK

---

**Input:**  $\mathcal{X}^0 \in \mathbb{C}^{\ell \times p \times n}$ ,  $\mathcal{A} \in \mathbb{C}^{m \times \ell \times n}$ ,  $\mathcal{B} \in \mathbb{C}^{m \times p \times n}$ , and probabilities  $p_0, \dots, p_{m-1}$  corresponding to each row slice of  $\mathcal{A}$   
**for**  $t = 0, 1, 2, \dots$  **do**  
    Sample  $i_t \sim p_i$   
     $\mathcal{X}^{t+1} = \mathcal{X}^t - \mathcal{A}_{i_t::}^* (\mathcal{A}_{i_t::} \mathcal{A}_{i_t::}^*)^{-1} (\mathcal{A}_{i_t::} \mathcal{X}^t - \mathcal{B}_{i_t::})$ .  
**Output:** last iterate  $\mathcal{X}^{t+1}$

---

Let  $\mathcal{P}_i = \mathcal{A}_{i::}^* (\mathcal{A}_{i::} \mathcal{A}_{i::}^*)^{-1} \mathcal{A}_{i::}$ . Under the assumption that  $\mathcal{A}_{i::} \mathcal{A}_{i::}^*$  is invertible, by Lemma 3,  $\mathcal{P}_i$  is an orthogonal projection onto the range of  $\mathcal{A}_{i::}$ . Consequently, at each iteration, the current iterate  $\mathcal{X}^t$  is projected onto the solution space of the sub-sampled system  $\mathcal{A}_{i_t::} \mathcal{X} = \mathcal{B}_{i_t::}$ . Note that this is the natural analogue of the MRK update, which projects the current iterate  $x^t$  onto the solution space of  $\mathbf{A}_{i_t} x = b_{i_t}$ .

Recall the MRK update given in Equation (1). The multiplication by  $(\mathcal{A}_{i_t::} \mathcal{A}_{i_t::}^*)^{-1}$  in the TRK update serves an analogous role to normalization by the squared row norms,  $\|\mathbf{A}_{i_t}\|^2$ , in the MRK update. The following assumption insures that the tensor  $\mathcal{A}_{i_t::} \mathcal{A}_{i_t::}^*$  is invertible so that the iterates are well defined.

**Assumption 1.** Assume that  $\mathcal{A}_{i::} \mathcal{A}_{i::}^*$  is invertible.

Note that in order for  $\mathcal{A}_{i::} \mathcal{A}_{i::}^*$  to be invertible,  $\text{diag}(\mathbf{F}_n \text{bcirc}(\mathcal{A}_{i::} \mathcal{A}_{i::}^*) \mathbf{F}_n^*) = \text{diag}(\mathbf{D})$  must contain no non-zero entries. If the matrix  $\text{bcirc}(\mathcal{A}_{i::} \mathcal{A}_{i::}^*)$  is invertible, then the tensor  $\mathcal{A}_{i::} \mathcal{A}_{i::}^*$  is also and its inverse can be calculated explicitly as follows.

**Lemma 5.** The inverse of  $\mathcal{A}_{i::} \mathcal{A}_{i::}^*$  under the  $t$ -product is

$$(\mathcal{A}_{i::} \mathcal{A}_{i::}^*)^{-1} = \text{fold} \left( \frac{1}{\sqrt{n}} \mathbf{F}_n^* \text{diag}(\mathbf{D}^{-1}) \right), \quad (7)$$

where  $\mathbf{F}_n$  is the  $n \times n$  Discrete Fourier Transform (DFT) matrix and  $\mathbf{D}$  is a diagonal matrix such that  $\text{bcirc}(\mathcal{A}_{i::} \mathcal{A}_{i::}^*) = \mathbf{F}_n^* \mathbf{D} \mathbf{F}_n$ .

*Proof.* The inverse of  $\mathcal{A}_{i::} \mathcal{A}_{i::}^*$  is given by the tube fiber  $\mathcal{W}$  that satisfies

$$\mathcal{A}_{i::} \mathcal{A}_{i::}^* \mathcal{W} = \text{fold}(\text{bcirc}(\mathcal{A}_{i::} \mathcal{A}_{i::}^*) \text{unfold}(\mathcal{W})) = \mathcal{I}.$$

Since  $\mathcal{A}_{i::} \mathcal{A}_{i::}^* \in \mathbb{C}^{1 \times 1 \times n}$  is a tube fiber,  $\text{bcirc}(\mathcal{A}_{i::} \mathcal{A}_{i::}^*)$  is a circulant matrix. Circulant matrices are diagonalizable by the DFT given by  $\mathbf{F}_n$ , and we can thus write  $\text{bcirc}(\mathcal{A}_{i::} \mathcal{A}_{i::}^*) = \mathbf{F}_n^* \mathbf{D} \mathbf{F}_n$  for some diagonal matrix  $\mathbf{D}$ . Inverting this, we have  $[\text{bcirc}(\mathcal{A}_{i::} \mathcal{A}_{i::}^*)]^{-1} = \mathbf{F}_n^* \mathbf{D}^{-1} \mathbf{F}_n$ .

Thus

$$\text{unfold}(\mathcal{W}) = [\text{bcirc}(\mathcal{A}_{i::} \mathcal{A}_{i::}^*)]^{-1} \text{unfold}(\mathcal{I}) = \mathbf{F}_n^* \mathbf{D}^{-1} \mathbf{F}_n \text{unfold}(\mathcal{I}).$$

Using the definition of the DFT matrix,

$$\mathbf{F}_n \text{unfold}(\mathcal{I}) = \mathbf{F}_n \begin{pmatrix} 1 \\ 0 \\ \vdots \\ 0 \end{pmatrix} = \frac{1}{\sqrt{n}} \begin{pmatrix} 1 \\ 1 \\ \vdots \\ 1 \end{pmatrix}.$$

Thus,

$$\mathcal{W} = \text{fold} \left( \frac{1}{\sqrt{n}} \mathbf{F}_n^* \text{diag}(\mathbf{D}^{-1}) \right).$$

□

## 4 Convergence

We demonstrate that the TRK method given by the update in Equation (6) satisfies a convergence result analogous to that of the matrix, vector setting. Theorem 6 shows that in expectation, the TRK algorithm will converge linearly to the solution of a consistent tensor system if

$$\rho := 1 - \sigma_{\min}(\mathbb{E}[\text{bcirc}(\mathcal{P}_i)]) < 1.$$

The constant  $\rho$  is often referred to as the *contraction coefficient*. To show that this term is indeed less than one, we take advantage of the fact that the t-product can be computed in Fourier space. This analysis is presented in Section 5. In this section, the TRK algorithm is analyzed with a more classical approach for Kaczmarz-type algorithms and the result is compared to the standard MRK convergence guarantee.

**Theorem 6.** *Let  $\mathcal{X}^*$  be such that  $\mathcal{A}\mathcal{X}^* = \mathcal{B}$  and  $\mathcal{X}^t$  be the  $t^{\text{th}}$  approximation of  $\mathcal{X}^*$  given by the updates of Equation (6) with initial iterate  $\mathcal{X}^0$  and indices  $i$  sampled independently from a probability distribution  $\mathcal{D}$  at each iteration. Denote the orthogonal projection  $\mathcal{P}_i = \mathcal{A}_{i::}^* (\mathcal{A}_{i::} \mathcal{A}_{i::}^*)^{-1} \mathcal{A}_{i::}$ . The expected error at the  $t + 1^{\text{st}}$  iteration satisfies*

$$\mathbb{E} \left[ \left\| \mathcal{X}^{t+1} - \mathcal{X}^* \right\|_F^2 \middle| \mathcal{X}^0 \right] \leq (1 - \sigma_{\min}(\mathbb{E}[\text{bcirc}(\mathcal{P}_i)]))^{t+1} \left\| \mathcal{X}^0 - \mathcal{X}^* \right\|_F^2,$$

where the expectation is taken over the probability distribution  $\mathcal{D}$ ,  $\sigma_{\min}(\mathbf{M})$  denotes the smallest singular value of  $\mathbf{M}$ , and  $\|\mathcal{M}\|_F^2$  is the sum of squared entries of the tensor  $\mathcal{M}$ .

The proof of Theorem 6 mirrors the standard analysis of MRK making use of the linear algebra mimetic properties of the t-product. More specifically, the proof proceeds as follows. First, we show that the expected error at the  $t^{\text{th}}$  iteration is bounded above by the error from the previous iteration minus a projected error term using a tensor Pythagorean theorem. Then, a lower bound on the norm of the projected error is obtained to lead to the desired result. The proof of Theorem 6 is provided here and more technical components that extend simple properties for tensors are deferred to the appendix.

*Proof.* Let  $\mathcal{X}^*$  be such that  $\mathcal{A}\mathcal{X}^* = \mathcal{B}$ . Subtracting  $\mathcal{X}^*$  from both sides of the TRK update given in Equation (6),

$$\begin{aligned}\mathcal{X}^{t+1} - \mathcal{X}^* &= \mathcal{X}^t - \mathcal{X}^* - \mathcal{A}_{i_t::}^* (\mathcal{A}_{i_t::} \mathcal{A}_{i_t::}^*)^{-1} (\mathcal{A}_{i_t::} \mathcal{X}^t - \mathcal{B}_{i_t::}) \\ &= \mathcal{X}^t - \mathcal{X}^* - \mathcal{A}_{i_t::}^* (\mathcal{A}_{i_t::} \mathcal{A}_{i_t::}^*)^{-1} \mathcal{A}_{i_t::} (\mathcal{X}^t - \mathcal{X}^*) \\ &= (\mathcal{I} - \mathcal{P}_{i_t}) (\mathcal{X}^t - \mathcal{X}^*).\end{aligned}$$

To simplify and condense notation, we will use  $\mathcal{E}^t = \mathcal{X}^t - \mathcal{X}^*$  to represent the error at iteration  $t$ . Taking the Frobenius norm of the equality above,

$$\|\mathcal{E}^{t+1}\|_F^2 = \|(\mathcal{I} - \mathcal{P}_{i_t}) \mathcal{E}^t\|_F^2.$$

As holds for orthogonal matrix projections, we can decompose this error as

$$\|(\mathcal{I} - \mathcal{P}_{i_t}) \mathcal{E}^t\|_F^2 = \|\mathcal{E}^t\|_F^2 - \|\mathcal{P}_{i_t} \mathcal{E}^t\|_F^2 \quad (8)$$

using the Pythagorean theorem (see Lemma 12).

Thus, Equation (8) holds and

$$\|\mathcal{E}^{t+1}\|_F^2 = \|\mathcal{E}^t\|_F^2 - \|\mathcal{P}_{i_t} \mathcal{E}^t\|_F^2.$$

Since the distribution from which the rows are sampled is fixed for all iterations, we drop the dependence on the iteration  $t$  when taking expectations. Taking the expectation over all row slice indices  $i$ ,

$$\mathbb{E} \left[ \|\mathcal{E}^{t+1}\|_F^2 \middle| \mathcal{X}^t \right] = \|\mathcal{E}^t\|_F^2 - \mathbb{E} \left[ \|\mathcal{P}_i \mathcal{E}^t\|_F^2 \right]. \quad (9)$$

Note that

$$\|\mathcal{P}_i \mathcal{E}^t\|_F^2 = \|\text{bcirc}(\mathcal{P}_i) \text{unfold}(\mathcal{E}^t)\|_F^2 = \sum_{j=1}^p \left\| \text{bcirc}(\mathcal{P}_i) \text{unfold}(\mathcal{E}^t)_{:j} \right\|_2^2.$$

Now, since  $\text{bcirc}(\mathcal{P}_i)$  is an orthogonal projection,

$$\begin{aligned}\mathbb{E} \left[ \|\mathcal{P}_i \mathcal{E}^t\|_F^2 \right] &= \sum_{j=1}^p \mathbb{E} \left[ \langle \text{bcirc}(\mathcal{P}_i) \text{unfold}(\mathcal{E}^t)_{:j}, \text{bcirc}(\mathcal{P}_i) \text{unfold}(\mathcal{E}^t)_{:j} \rangle \right] \\ &= \sum_{j=1}^p \langle \mathbb{E} [\text{bcirc}(\mathcal{P}_i)] \text{unfold}(\mathcal{E}^t)_{:j}, \text{unfold}(\mathcal{E}^t)_{:j} \rangle.\end{aligned} \quad (10)$$

Since  $\mathbb{E} [\text{bcirc}(\mathcal{P}_i)]$  is symmetric,

$$\begin{aligned}\mathbb{E} \left[ \|\mathcal{P}_i \mathcal{E}^t\|_F^2 \right] &\geq \sigma_{\min}(\mathbb{E} [\text{bcirc}(\mathcal{P}_i)]) \sum_{j=1}^p \left\| \text{unfold}(\mathcal{E}^t)_{:j} \right\|_2^2 \\ &\geq \sigma_{\min}(\mathbb{E} [\text{bcirc}(\mathcal{P}_i)]) \sum_{j=1}^p \|\mathcal{E}_{:j}^t\|_F^2 \\ &\geq \sigma_{\min}(\mathbb{E} [\text{bcirc}(\mathcal{P}_i)]) \|\mathcal{E}^t\|_F^2.\end{aligned}$$

Making this substitution in Equation (9), we then have

$$\mathbb{E} \left[ \|\mathcal{E}^{t+1}\|_F^2 \middle| \mathcal{X}^t \right] \leq (1 - \sigma_{\min}(\mathbb{E}[\text{bcirc}(\mathcal{P}_i)])) \|\mathcal{E}^t\|_F^2.$$

Since the row slice indices  $i$  are sampled independently, the conditional expectation can be iterated to obtain,

$$\mathbb{E} \left[ \|\mathcal{E}^{t+1}\|_F^2 \middle| \mathcal{X}^0 \right] \leq (1 - \sigma_{\min}(\mathbb{E}[\text{bcirc}(\mathcal{P}_i)]))^{t+1} \|\mathcal{E}^0\|_F^2.$$

□

The convergence guarantee of Theorem 6 is analogous to that of [34] for MRK. If rows are sampled with probabilities proportional to the squared row norms of  $\mathbf{A}$ , the expected approximation error for iterates of MRK is upper bounded as:

$$\begin{aligned} \mathbb{E} \left[ \|x^{t+1} - x^*\|^2 \middle| x^0 \right] &\leq \left( 1 - \sigma_{\min} \left( \frac{\mathbb{E}[\mathbf{A}_{i:} \mathbf{A}_{i:}^*]}{\|\mathbf{A}\|_F^2} \right) \right)^{t+1} \|x^0 - x^*\|^2 \\ &\leq \left( 1 - \frac{\sigma_{\min}(\mathbf{A}^* \mathbf{A})}{\|\mathbf{A}\|_F^2} \right)^{t+1} \|x^0 - x^*\|^2. \end{aligned}$$

Both the TRK and MRK convergence guarantees depend on the minimal singular value of the expectation over the possible projections onto the rows or row slices for the matrix and tensor versions respectively.

## 5 Analysis of TRK in the Fourier domain

The t-product can be computed efficiently using the Fast Fourier Transform (FFT), since circulant matrices are diagonalized by the DFT. Similarly, we can analyze the convergence of TRK in the Fourier domain and capitalize on the resulting block-diagonal structure. In this section, we present a convergence analysis in the Fourier domain to derive a more interpretable convergence guarantee for TRK. We describe how the TRK update can be performed efficiently in the Fourier domain and additionally demonstrate that TRK is equivalent to performing block MRK on the linear system in the Fourier domain.

### 5.1 Notation and preliminary facts

We first introduce some additional notation and basic facts that will be used throughout this section. The notation and definitions are adopted from [17]. Let  $\mathcal{M} \in \mathbb{C}^{m \times \ell \times n}$  and  $\widehat{\mathcal{M}}$  denote the tensor resulting from applying the DFT matrix to each of the tube fibers of  $\mathcal{M}$ . This operation is referred to in

previous literature as a *mode-3 FFT*. Fact 2 of [17], guarantees that

$$\text{bdiag}(\widehat{\mathcal{M}}) := (\mathbf{F}_n \otimes \mathbf{I}_m) \text{bcirc}(\mathcal{M}) (\mathbf{F}_n^* \otimes \mathbf{I}_\ell) = \begin{pmatrix} \widehat{\mathbf{M}}_0 & & & \\ & \widehat{\mathbf{M}}_1 & & \\ & & \ddots & \\ & & & \widehat{\mathbf{M}}_{n-1} \end{pmatrix}, \quad (11)$$

where  $\widehat{\mathbf{M}}_k$  is the  $k^{\text{th}}$  frontal face of  $\widehat{\mathcal{M}}$ ,  $\otimes$  denotes the Kronecker product,  $\mathbf{F}_n$  is the  $n \times n$  DFT matrix, and  $\text{bdiag}(\widehat{\mathcal{M}})$  is the block diagonal matrix formed by the frontal faces of  $\widehat{\mathcal{M}}$ .

We now present several facts which hold true for tensors under the t-product. They will be useful for performing calculations in the Fourier domain.

**Fact 7.** *For tensors  $\mathcal{A}$  and  $\mathcal{B}$  the following holds:*

$$\text{bdiag}(\widehat{\mathcal{A}\mathcal{B}}) = \text{bdiag}(\widehat{\mathcal{A}}) \text{bdiag}(\widehat{\mathcal{B}}).$$

*Proof.* Let  $\mathcal{A} \in \mathbb{C}^{m \times \ell \times n}$  and  $\mathcal{B} \in \mathbb{C}^{\ell \times p \times n}$ , then

$$\begin{aligned} \text{bdiag}(\widehat{\mathcal{A}\mathcal{B}}) &\stackrel{(11)}{=} (\mathbf{F}_n \otimes \mathbf{I}_m) \text{bcirc}(\mathcal{A}\mathcal{B}) (\mathbf{F}_n^* \otimes \mathbf{I}_p) \\ &\stackrel{\text{Fact 1}}{=} (\mathbf{F}_n \otimes \mathbf{I}_m) \text{bcirc}(\mathcal{A}) \text{bcirc}(\mathcal{B}) (\mathbf{F}_n^* \otimes \mathbf{I}_p) \\ &= (\mathbf{F}_n \otimes \mathbf{I}_m) \text{bcirc}(\mathcal{A}) (\mathbf{F}_n^* \otimes \mathbf{I}_\ell) (\mathbf{F}_n \otimes \mathbf{I}_\ell) \text{bcirc}(\mathcal{B}) (\mathbf{F}_n^* \otimes \mathbf{I}_p) \\ &\stackrel{(11)}{=} \text{bdiag}(\widehat{\mathcal{A}}) \text{bdiag}(\widehat{\mathcal{B}}). \end{aligned}$$

□

**Fact 8.** *Addition and  $\widehat{\cdot}$  are commutative*

$$\widehat{\mathcal{A} + \mathcal{B}} = \widehat{\mathcal{A}} + \widehat{\mathcal{B}}.$$

*Proof.* Let  $\mathcal{A} \in \mathbb{C}^{m \times \ell \times n}$  and  $\mathcal{B} \in \mathbb{C}^{m \times \ell \times n}$ , then

$$\begin{aligned} \text{bdiag}(\widehat{\mathcal{A} + \mathcal{B}}) &\stackrel{(11)}{=} (\mathbf{F}_n \otimes \mathbf{I}_m) \text{bcirc}(\mathcal{A} + \mathcal{B}) (\mathbf{F}_n^* \otimes \mathbf{I}_\ell) \\ &= (\mathbf{F}_n \otimes \mathbf{I}_m) (\text{bcirc}(\mathcal{A}) + \text{bcirc}(\mathcal{B})) (\mathbf{F}_n^* \otimes \mathbf{I}_\ell) \\ &= (\mathbf{F}_n \otimes \mathbf{I}_m) \text{bcirc}(\mathcal{A}) (\mathbf{F}_n^* \otimes \mathbf{I}_\ell) + (\mathbf{F}_n \otimes \mathbf{I}_m) \text{bcirc}(\mathcal{B}) (\mathbf{F}_n^* \otimes \mathbf{I}_\ell) \\ &\stackrel{(11)}{=} \text{bdiag}(\widehat{\mathcal{A}}) + \text{bdiag}(\widehat{\mathcal{B}}). \end{aligned}$$

□

**Fact 9.** *The conjugate transpose commutes with  $\text{bdiag}(\widehat{\cdot})$ ,*

$$\text{bdiag}(\widehat{\mathcal{M}^*}) = \text{bdiag}(\widehat{\mathcal{M}})^*.$$

*Additionally, if  $\text{bcirc}(\mathcal{M})$  is symmetric,  $\text{bdiag}(\widehat{\mathcal{M}})$  is also symmetric.*

*Proof.* Let  $\mathcal{M} \in \mathbb{C}^{m \times \ell \times n}$ . Then

$$\begin{aligned} \text{bdiag}(\widehat{\mathcal{M}}^*) &\stackrel{(11)}{=} (\mathbf{F}_n \otimes \mathbf{I}_\ell) \text{bcirc}(\mathcal{M}^*) (\mathbf{F}_n^* \otimes \mathbf{I}_m) \\ &\stackrel{\text{Fact 2}}{=} (\mathbf{F}_n \otimes \mathbf{I}_\ell) \text{bcirc}(\mathcal{M})^* (\mathbf{F}_n^* \otimes \mathbf{I}_m) \\ &= [(\mathbf{F}_n \otimes \mathbf{I}_m) \text{bcirc}(\mathcal{M}) (\mathbf{F}_n^* \otimes \mathbf{I}_\ell)]^* \\ &\stackrel{(11)}{=} \text{bdiag}(\widehat{\mathcal{M}})^*. \end{aligned}$$

To see that  $\text{bdiag}(\widehat{\mathcal{M}})$  is also symmetric when  $\text{bcirc}(\mathcal{M})$  is symmetric, note that

$$\text{bdiag}(\widehat{\mathcal{M}})^* \stackrel{(11)}{=} [(\mathbf{F}_n \otimes \mathbf{I}_m) \text{bcirc}(\mathcal{M}) (\mathbf{F}_n^* \otimes \mathbf{I}_n)]^*.$$

□

**Fact 10.** *The inverse commutes with  $\text{bdiag}(\widehat{\cdot})$ ,*

$$\text{bdiag}(\widehat{\mathcal{M}^{-1}}) = \text{bdiag}(\widehat{\mathcal{M}})^{-1}.$$

*Proof.* Let  $\mathcal{M} \in \mathbb{C}^{m \times m \times n}$ . Note that  $\text{bcirc}(\mathcal{I}_m) = \mathbf{I}_{mn}$ . Using Fact 1 and Equation (11),

$$\begin{aligned} \text{bdiag}(\widehat{\mathcal{M}^{-1}}) \text{bdiag}(\widehat{\mathcal{M}}) &\stackrel{(11)}{=} (\mathbf{F}_n \otimes \mathbf{I}_m) \text{bcirc}(\mathcal{M}^{-1}) (\mathbf{F}_n^* \otimes \mathbf{I}_m) (\mathbf{F}_n \otimes \mathbf{I}_m) \text{bcirc}(\mathcal{M}) (\mathbf{F}_n^* \otimes \mathbf{I}_m) \\ &= (\mathbf{F}_n \otimes \mathbf{I}_m) \text{bcirc}(\mathcal{M}^{-1}) \text{bcirc}(\mathcal{M}) (\mathbf{F}_n^* \otimes \mathbf{I}_m) \\ &\stackrel{\text{Fact 1}}{=} (\mathbf{F}_n \otimes \mathbf{I}_m) \text{bcirc}(\mathcal{I}_m) (\mathbf{F}_n^* \otimes \mathbf{I}_m) \\ &= \mathbf{I}_{mn}. \end{aligned}$$

Analogously, one can show  $\text{bdiag}(\widehat{\mathcal{M}}) \text{bdiag}(\widehat{\mathcal{M}^{-1}}) = \mathbf{I}_{mn}$ .

□

## 5.2 A more interpretable convergence guarantee

Using Fact 2 of [17], we can derive a more interpretable convergence guarantee in terms of the tensor  $\mathcal{A}$ . Specifically, assuming that the indices  $i_t$  are sampled uniformly at random at each iteration, we can restate Theorem 6 as follows.

**Theorem 11.** *Let  $\mathcal{X}^*$  be such that  $\mathcal{A}\mathcal{X}^* = \mathcal{B}$  and  $\mathcal{X}^t$  be the  $t^{\text{th}}$  approximation of  $\mathcal{X}^*$  given by the updates of Equation (6) with initial iterate  $\mathcal{X}^0$  and indices  $i_t \in [m-1]$  sampled uniformly at random at each iteration. The expected error at the  $(t+1)^{\text{st}}$  iteration satisfies*

$$\mathbb{E} \left[ \|\mathcal{X}^{t+1} - \mathcal{X}^*\|_F^2 \middle| \mathcal{X}^0 \right] \leq \left( 1 - \min_{k \in [n-1]} \frac{\sigma_{\min}^2(\widehat{\mathcal{A}}_k)}{m \|\widehat{\mathcal{A}}_k\|_{\infty,2}^2} \right)^{t+1} \|\mathcal{X}^0 - \mathcal{X}^*\|_F^2,$$

where  $\|\cdot\|_{\infty,2}$  is as defined in Equation (14),  $\widehat{\mathcal{A}}_k$  is the  $k^{\text{th}}$  frontal slice of  $\widehat{\mathcal{A}}$ , and  $\sigma_{\min}(\cdot)$  denotes the smallest singular value.

*Proof.* Let  $\widehat{\mathcal{P}}_i$  be the tensor formed by applying FFTs to each tube fiber of  $\mathcal{P}_i = \mathcal{A}_{i::}^* (\mathcal{A}_{i::} \mathcal{A}_{i::}^*)^{-1} \mathcal{A}_{i::}$ . By Equation (11), we have that

$$\text{bdiag}(\widehat{\mathcal{P}}_i) = (\mathbf{F}_n \otimes \mathbf{I}_\ell) \text{bcirc}(\mathcal{P}_i) (\mathbf{F}_n^* \otimes \mathbf{I}_\ell),$$

is a block diagonal matrix with blocks  $(\widehat{\mathbf{P}}_i)_k$ , where  $(\widehat{\mathbf{P}}_i)_k$  is the  $k^{\text{th}}$  frontal slice of the tensor  $\widehat{\mathcal{P}}_i$ . We note that the projected error in Equation (10) can be rewritten as

$$\begin{aligned} \mathbb{E} \left[ \|\mathcal{P}_i \mathcal{E}^t\|_F^2 \right] &= \sum_{j=1}^p \langle \mathbb{E}[\text{bcirc}(\mathcal{P}_i)] \text{unfold}(\mathcal{E}^t)_{:,j}, \text{unfold}(\mathcal{E}^t)_{:,j} \rangle \\ &= \sum_{j=1}^p \mathbb{E} \left[ \langle (\mathbf{F}_n \otimes \mathbf{I}_\ell) \text{bcirc}(\mathcal{P}_i) (\mathbf{F}_n^* \otimes \mathbf{I}_\ell) (\mathbf{F}_n \otimes \mathbf{I}_\ell) \text{unfold}(\mathcal{E}^t)_{:,j}, (\mathbf{F}_n \otimes \mathbf{I}_\ell) \text{unfold}(\mathcal{E}^t)_{:,j} \rangle \right] \\ &= \sum_{j=1}^p \mathbb{E} \left[ \langle \text{bdiag}(\widehat{\mathcal{P}}_i) (\mathbf{F}_n \otimes \mathbf{I}_\ell) \text{unfold}(\mathcal{E}^t)_{:,j}, (\mathbf{F}_n \otimes \mathbf{I}_\ell) \text{unfold}(\mathcal{E}^t)_{:,j} \rangle \right]. \end{aligned}$$

Now, since  $\mathbb{E}[\text{bdiag}(\widehat{\mathcal{P}}_i)]$  is symmetric by Fact 9,

$$\mathbb{E} \left[ \|\mathcal{P}_i \mathcal{E}^t\|_F^2 \right] \geq \sigma_{\min} \left( \mathbb{E}[\text{bdiag}(\widehat{\mathcal{P}}_i)] \right) \|(\mathbf{F}_n \otimes \mathbf{I}_\ell) \text{unfold}(\mathcal{E}^t)\|_F^2. \quad (12)$$

Note that,

$$\begin{aligned} \|(\mathbf{F}_n \otimes \mathbf{I}_\ell) \text{unfold}(\mathcal{E}^t)\|_F^2 &= \sum_{j=1}^p \langle (\mathbf{F}_n \otimes \mathbf{I}_\ell) \text{unfold}(\mathcal{E}^t)_{:,j}, (\mathbf{F}_n \otimes \mathbf{I}_\ell) \text{unfold}(\mathcal{E}^t)_{:,j} \rangle \\ &= \sum_{j=1}^p \langle \text{unfold}(\mathcal{E}^t)_{:,j}, \text{unfold}(\mathcal{E}^t)_{:,j} \rangle \\ &= \|\text{unfold}(\mathcal{E}^t)\|_F^2 \\ &= \|\mathcal{E}^t\|_F^2. \end{aligned}$$

Since  $\text{bdiag}(\widehat{\mathcal{P}}_i)$  is block diagonal,

$$\sigma_{\min} \left( \mathbb{E}[\text{bdiag}(\widehat{\mathcal{P}}_i)] \right) = \min_{k \in [n-1]} \sigma_{\min} \left( \mathbb{E}[(\widehat{\mathbf{P}}_i)_k] \right).$$

Factoring  $\text{bdiag}(\widehat{\mathcal{P}}_i)$ ,

$$\begin{aligned} \text{bdiag}(\widehat{\mathcal{P}}_i) &\stackrel{\text{Fact 7}}{=} \text{bdiag}(\widehat{\mathcal{A}}_{i::}^*) \text{bdiag}(\widehat{(\mathcal{A}_{i::}\mathcal{A}_{i::}^*)^{-1}}) \text{bdiag}(\widehat{\mathcal{A}}_{i::}) \\ &\stackrel{\text{Facts 9-10}}{=} \text{bdiag}(\widehat{\mathcal{A}}_{i::})^* \text{bdiag}(\widehat{\mathcal{A}_{i::}\mathcal{A}_{i::}^*})^{-1} \text{bdiag}(\widehat{\mathcal{A}}_{i::}) \\ &\stackrel{\text{Fact 7}}{=} \text{bdiag}(\widehat{\mathcal{A}}_{i::})^* \left[ \text{bdiag}(\widehat{\mathcal{A}}_{i::}) \text{bdiag}(\widehat{\mathcal{A}}_{i::}^*) \right]^{-1} \text{bdiag}(\widehat{\mathcal{A}}_{i::}). \end{aligned}$$

Noting that  $\text{bdiag}(\widehat{\mathcal{A}}_{i::}) \text{bdiag}(\widehat{\mathcal{A}}_{i::}^*)$  is a diagonal matrix, one can see that  $(\widehat{\mathbf{P}}_i)_k$  is the projection onto  $(\widehat{\mathcal{A}}_{i::})_k$  by rewriting the  $k^{\text{th}}$  frontal face of  $\widehat{\mathcal{P}}_i$  as

$$(\widehat{\mathbf{P}}_i)_k = \frac{(\widehat{\mathcal{A}}_{i::})_k^* (\widehat{\mathcal{A}}_{i::})_k}{(\widehat{\mathcal{A}_{i::}\mathcal{A}_{i::}^*})_k}.$$

We can thus rewrite Equation (12) as

$$\mathbb{E} \left[ \|\mathcal{P}_i \mathcal{E}^t\|_F^2 \right] \geq \min_{k \in [n-1]} \sigma_{\min} \left( \mathbb{E} \left[ \frac{(\widehat{\mathcal{A}}_{i::})_k^* (\widehat{\mathcal{A}}_{i::})_k}{(\widehat{\mathcal{A}_{i::}\mathcal{A}_{i::}^*})_k} \right] \right) \|\mathcal{E}^t\|_F^2. \quad (13)$$

The expectation of Equation (12) can now be calculated explicitly. For simplicity, we assume that the row indices  $i$  are sampled uniformly. As in MRK extensions and literature, many other sampling distributions could be used.

To derive a lower bound for the smallest singular value in Equation (13), define

$$\|\widehat{\mathcal{A}}_k\|_{\infty,2}^2 := \max_i \left[ (\widehat{\mathcal{A}_{i::}\mathcal{A}_{i::}^*})_k \right]. \quad (14)$$

The values  $(\widehat{\mathcal{A}_{i::}\mathcal{A}_{i::}^*})_k$  are necessarily positive for all  $k \in [n-1]$  under Assumption 1 as

$$\begin{aligned} (\widehat{\mathcal{A}_{i::}\mathcal{A}_{i::}^*})_k &= \text{bdiag}(\widehat{\mathcal{A}_{i::}\mathcal{A}_{i::}^*})_{kk} \\ &= \text{bdiag}(\widehat{\mathcal{A}}_{i::})_k \text{bdiag}(\widehat{\mathcal{A}}_{i::}^*)_k \\ &= (\mathbf{F}_n)_{k:} \text{bcirc}(\mathcal{A}_{i::}) \text{bcirc}(\mathcal{A}_{i::}^*) (\mathbf{F}_n)_{k:}^* \\ &= (\mathbf{F}_n)_{k:} \text{bcirc}(\mathcal{A}_{i::}) \text{bcirc}(\mathcal{A}_{i::})^* (\mathbf{F}_n)_{k:}^* \\ &= \|\text{bcirc}(\mathcal{A}_{i::})^* (\mathbf{F}_n)_{k:}^*\|_2^2. \end{aligned}$$



Now, it can be easily verified that

$$\begin{aligned} \sigma_{\min} \left( \mathbb{E} \left[ \frac{(\widehat{\mathcal{A}}_{i::})^* (\widehat{\mathcal{A}}_{i::})_k}{(\widehat{\mathcal{A}}_{i::} \widehat{\mathcal{A}}_{i::}^*)_k} \right] \right) &\geq \sigma_{\min} \left( \frac{1}{m} \sum_{i=0}^{m-1} \frac{(\widehat{\mathcal{A}}_{i::})^* (\widehat{\mathcal{A}}_{i::})_k}{\|\widehat{\mathcal{A}}_k\|_{\infty,2}^2} \right) \\ &= \frac{\sigma_{\min}^2(\widehat{\mathcal{A}}_k)}{m \|\widehat{\mathcal{A}}_k\|_{\infty,2}^2}. \end{aligned}$$

The projected error of Equation (13) then becomes

$$\mathbb{E} \left[ \|\mathcal{P}_i \mathcal{E}^t\|_F^2 \right] \geq \min_{k \in [n-1]} \frac{\sigma_{\min}^2(\widehat{\mathcal{A}}_k)}{m \|\widehat{\mathcal{A}}_k\|_{\infty,2}^2} \|\mathcal{E}^t\|_F^2, \quad (15)$$

leading to a contraction coefficient of

$$\rho = 1 - \min_{k \in [n-1]} \frac{\sigma_{\min}^2(\widehat{\mathcal{A}}_k)}{m \|\widehat{\mathcal{A}}_k\|_{\infty,2}^2}. \quad (16)$$

We can thus rewrite the guarantee in Theorem 6 for uniform random sampling of the row indices  $i$  as

$$\mathbb{E} \left[ \|\mathcal{X}^{t+1} - \mathcal{X}^*\|_F^2 \middle| \mathcal{X}^0 \right] \leq \left( 1 - \min_{k \in [n-1]} \frac{\sigma_{\min}^2(\widehat{\mathcal{A}}_k)}{m \|\widehat{\mathcal{A}}_k\|_{\infty,2}^2} \right)^{t+1} \|\mathcal{X}^0 - \mathcal{X}^*\|_F^2. \quad (17)$$

□

### 5.3 Equivalence of TRK and block MRK applied in the Fourier domain

In this section, we observe a connection between the proposed TRK method and the previously studied block MRK algorithm [25]. This analysis helps to further bridge the understanding of connections between TRK and MRK. In block MRK, one projects the current iterate onto the solution space of a set of constraints (set of rows of the linear system) as opposed to the solution space with respect to a single row. In practice, block MRK can lead to a significant speed up over MRK [25].

Here we show the equivalence of TRK and block MRK performed in the Fourier domain with specific block partitions and remark on the convergence rate implications in the block MRK setting. Using Equation (11), the tensor

linear system Equation (3) can be rewritten as:

$$\begin{pmatrix} \hat{\mathcal{A}}_0 & & & \\ & \hat{\mathcal{A}}_1 & & \\ & & \ddots & \\ & & & \hat{\mathcal{A}}_{n-1} \end{pmatrix} \begin{pmatrix} \hat{\mathcal{X}}_0 \\ \hat{\mathcal{X}}_1 \\ \vdots \\ \hat{\mathcal{X}}_{n-1} \end{pmatrix} = \begin{pmatrix} \hat{\mathcal{B}}_0 \\ \hat{\mathcal{B}}_1 \\ \vdots \\ \hat{\mathcal{B}}_{n-1} \end{pmatrix}. \quad (18)$$

The system shown in Equation (18) can be solved using block MRK such that the resulting iterate is equivalent to the TRK iterate in the following way. Let

$$\tau_i = \{km + i \mid k \in [n-1]\}, \quad (19)$$

denote in set of indices corresponding to a randomly selected block of the measurement matrix in Equation (18). This choice of  $\tau_i$  corresponds to selecting the  $i^{\text{th}}$  row of each  $\hat{\mathcal{A}}_k$  in  $\text{bdiag}(\hat{\mathcal{A}})$ , i.e., each row of  $\hat{\mathcal{A}}_{i::}$  appears along the diagonal of  $\text{bdiag}(\hat{\mathcal{A}})_{\tau_i}$  and therefore,  $\text{bdiag}(\hat{\mathcal{A}})_{\tau_i} = \text{bdiag}(\hat{\mathcal{A}}_{i::})$ .

For a randomly selected row index  $i_t \in [m-1]$ , the block MRK update for Equation (18) is aptly written as:

$$\begin{aligned} \text{unfold}(\hat{\mathcal{X}}^{t+1}) &= \text{unfold}(\hat{\mathcal{X}}^t) - \text{bdiag}(\hat{\mathcal{A}})_{\tau_{i_t}}^\dagger \left( \text{bdiag}(\hat{\mathcal{A}})_{\tau_{i_t}} \text{unfold}(\hat{\mathcal{X}}^t) - \text{unfold}(\hat{\mathcal{B}})_{\tau_{i_t}} \right) \\ &= \text{unfold}(\hat{\mathcal{X}}^t) - \text{bdiag}(\hat{\mathcal{A}}_{i_t::})^\dagger \left( \text{bdiag}(\hat{\mathcal{A}}_{i_t::}) \text{unfold}(\hat{\mathcal{X}}^t) - \text{unfold}(\hat{\mathcal{B}})_{\tau_{i_t}} \right). \end{aligned} \quad (20)$$

Using Equation (11) and Facts 7-10, we can show

$$\begin{aligned} \text{bdiag}(\hat{\mathcal{A}}_{i_t::})^\dagger &= \text{bdiag}(\hat{\mathcal{A}}_{i_t::})^* \left( \text{bdiag}(\hat{\mathcal{A}}_{i_t::}) \text{bdiag}(\hat{\mathcal{A}}_{i_t::})^* \right)^{-1} \\ &= \text{bdiag}(\hat{\mathcal{A}}_{i_t::}^* (\hat{\mathcal{A}}_{i_t::} \hat{\mathcal{A}}_{i_t::}^*)^{-1}) \end{aligned}$$

Therefore, noting the following equalities and folding the right and left sides of the equation into tensors, we derive the iterate update for  $\hat{\mathcal{X}}^{t+1}$  from the block MRK update:

$$\begin{aligned} \text{unfold}(\hat{\mathcal{X}}^{t+1}) &= \text{unfold}(\hat{\mathcal{X}}^t) - \text{bdiag}(\hat{\mathcal{A}}_{i_t::}^* (\hat{\mathcal{A}}_{i_t::} \hat{\mathcal{A}}_{i_t::}^*)^{-1}) \left( \text{bdiag}(\hat{\mathcal{A}}_{i_t::}) \text{unfold}(\hat{\mathcal{X}}^t) - \text{unfold}(\hat{\mathcal{B}})_{\tau_{i_t}} \right) \\ &= \text{unfold}(\hat{\mathcal{X}}^t) - (\mathbf{F}_n \otimes \mathbf{I}_\ell) \text{unfold}(\hat{\mathcal{A}}_{i_t::}^* (\hat{\mathcal{A}}_{i_t::} \hat{\mathcal{A}}_{i_t::}^*)^{-1} (\hat{\mathcal{A}}_{i_t::} \hat{\mathcal{X}}^t - \hat{\mathcal{B}}_{i_t::})) \\ &= \text{unfold}(\hat{\mathcal{X}}^t) - \text{unfold}(\hat{\mathcal{A}}_{i_t::}^* (\hat{\mathcal{A}}_{i_t::} \hat{\mathcal{A}}_{i_t::}^*)^{-1} (\hat{\mathcal{A}}_{i_t::} \hat{\mathcal{X}}^t - \hat{\mathcal{B}}_{i_t::})) \\ &\Rightarrow \hat{\mathcal{X}}^{t+1} = \hat{\mathcal{X}}^t - \hat{\mathcal{A}}_{i_t::}^* (\hat{\mathcal{A}}_{i_t::} \hat{\mathcal{A}}_{i_t::}^*)^{-1} (\hat{\mathcal{A}}_{i_t::} \hat{\mathcal{X}}^t - \hat{\mathcal{B}}_{i_t::}). \end{aligned} \quad (21)$$

Since the FFT is applied to each tube fiber of  $\mathcal{A}$  independently,  $\widehat{\mathcal{A}_{i::}} = \widehat{\mathcal{A}_{i::}}$ . To see that Equation (21) is equivalent to Equation (6) one can use Facts 7-10 to show that  $\widehat{\mathcal{X}^{t+1}} = \widehat{\mathcal{X}^{t+1}}$ , that is taking the inverse FFT on the tubes of  $\widehat{\mathcal{X}^{t+1}}$  will return the TRK update Equation (6).

*Remark 1.* The contraction rate for block MRK applied to the linear system Equation (18) with iterates as shown in Equation (20) is

$$\rho_{\text{BRK}} = 1 - \frac{\sigma_{\min}^2(\text{bdiag}(\widehat{\mathcal{A}}))}{mn \max_i \lambda_{\max} \left( \text{bdiag}(\widehat{\mathcal{A}})_{\tau_i} \text{bdiag}(\widehat{\mathcal{A}})_{\tau_i}^* \right)}. \quad (22)$$

The contraction coefficient  $\rho_{\text{BRK}}$  is a direct result of the theoretical guarantees for block MRK shown in [25]. Note that due to the block-diagonal structure, the numerator of the second term of Equation (22) can be simplified to

$$\sigma_{\min}^2(\text{bdiag}(\widehat{\mathcal{A}})) = \min_{k \in [n-1]} \sigma_{\min}^2(\widehat{\mathcal{A}}_k).$$

Using the fact that  $\text{bdiag}(\widehat{\mathcal{A}})_{\tau_i} = \text{bdiag}(\widehat{\mathcal{A}}_{i::})$  along with Facts 7 and 9, it can be easily shown that  $\text{bdiag}(\widehat{\mathcal{A}})_{\tau_i} \text{bdiag}(\widehat{\mathcal{A}})_{\tau_i}^* = \text{bdiag}(\widehat{\mathcal{A}}_{i::} \widehat{\mathcal{A}}_{i::}^*)$ . Thus, the denominator of Equation (22) can be simplified to:

$$\begin{aligned} \max_i \lambda_{\max} \left( \text{bdiag}(\widehat{\mathcal{A}})_{\tau_i} \text{bdiag}(\widehat{\mathcal{A}})_{\tau_i}^* \right) &= \max_i \lambda_{\max} \left( \text{bdiag}(\widehat{\mathcal{A}}_{i::} \widehat{\mathcal{A}}_{i::}^*) \right) \\ &= \max_i \max_k \left[ \widehat{\mathcal{A}}_{i::} \widehat{\mathcal{A}}_{i::}^* \right]_k \\ &\stackrel{(14)}{=} \max_k \left\| \widehat{\mathcal{A}}_k \right\|_{\infty, 2}^2, \end{aligned}$$

where the norm in the last equality is as defined in Equation (14). Putting this all together, the contraction rate for block MRK applied to Equation (18) is

$$\rho_{\text{BRK}} = 1 - \frac{\min_k \sigma_{\min}^2(\widehat{\mathcal{A}}_k)}{mn \max_k \left\| \widehat{\mathcal{A}}_k \right\|_{\infty, 2}^2}. \quad (23)$$

Compared to the convergence rate derived for TRK in Theorem 11, the standard block MRK convergence guarantee is weaker (slower). The standard analysis for the convergence of block MRK is not restricted to block diagonal systems. Thus, although block MRK applied to Equation (18) with predetermined blocks  $\tau_i$  is equivalent to the proposed TRK update, the standard block MRK guarantee is weaker since the TRK analysis takes advantage of the block diagonal structure of the system in the Fourier domain.

*Remark 2.* The block-diagonal system in Equation (18) is highly parallelizable. Specifically, each component block of the system  $\widehat{\mathcal{A}}_k \widehat{\mathcal{X}}_k = \widehat{\mathcal{B}}_k$  for  $k \in [n-1]$

---

**Algorithm 2** Tensor RK computed in the Fourier domain

---

**Input:**  $\mathcal{X}^0 \in \mathbb{C}^{\ell \times p \times n}$ ,  $\mathcal{A} \in \mathbb{C}^{m \times \ell \times n}$ ,  $\mathcal{B} \in \mathbb{C}^{m \times p \times n}$ , and probabilities  $p_0, \dots, p_{m-1}$  corresponding to each row slice of  $\mathcal{A}$   
Compute  $\widehat{\mathcal{X}}^0, \widehat{\mathcal{A}}, \widehat{\mathcal{B}}$  as in Equation (11)  
**for**  $t = 0, 1, 2, \dots$  **do**  
    Sample  $i_t \sim p_i$   
    **for**  $k = 0, 1, \dots, n-1$  **do**  
         $\widehat{\mathcal{X}}^{t+1}_k = \widehat{\mathcal{X}}^t_k - \left(\widehat{\mathcal{A}}_{i_t:k}\right)^\dagger \left(\widehat{\mathcal{A}}_{i_t:k} \widehat{\mathcal{X}}^t_k - \widehat{\mathcal{B}}_{i_t:k}\right)$   
    Recover  $\mathcal{X}^{t+1}$  from  $\widehat{\mathcal{X}}^{t+1}$   
**Output:** last iterate  $\mathcal{X}^{t+1}$

---

can be solved independently. For  $m$  extremely large, however, loading a single  $\widehat{\mathcal{A}}_i$  into memory maybe be impossible. In such settings, a randomized iterative method such as TRK is advantageous. The block-diagonal structure of the subsampled system in the Fourier domain also allows the update for each component block to be computed in parallel.

Making use of the equivalence of TRK and block MRK in the Fourier domain, TRK can be implemented efficiently using methods for matrices as detailed in Algorithm 2. Note that Equation (20) can be reformulated as

$$\widehat{\mathcal{X}}^{t+1}_k = \widehat{\mathcal{X}}^t_k - \left(\widehat{\mathcal{A}}_{i_t:k}\right)^\dagger \left(\widehat{\mathcal{A}}_{i_t:k} \widehat{\mathcal{X}}^t_k - \widehat{\mathcal{B}}_{i_t:k}\right) \text{ for } k \in [n-1],$$

by making use of the block structure.

*Remark 3.* The equivalence between TRK and block MRK with blocks indexed by Equation (19) also reveal a straightforward analysis for the comparison of the computational complexity between TRK and MRK. The per iteration complexity of MRK using rows  $\mathbf{A}_{i:} \in \mathbb{R}^{1 \times \ell n}$  is  $\mathcal{O}(\ell n)$  and the per iteration complexity of TRK using rows  $\mathcal{A}_{i::} \in \mathbb{R}^{1 \times \ell \times n}$  is  $\mathcal{O}(\ell n^2)$ .

## 6 Experiments

In this section, we present numerical experiments comparing MRK and TRK. The implementation of the TRK algorithm used is as outlined in Algorithm 1, unless otherwise noted. First, we show empirically that with an increasing number of measurements  $m$ , the contraction coefficient for TRK is smaller than that of MRK indicating a stronger convergence guarantee. Next, we compare the performance of TRK with that of MRK applied to a matrix linear system where the memory complexity of the measurement matrix is preserved. Then, we move on to the setting in which one is given tensor measurements  $\mathcal{B}$  and compare the performance of TRK with that of MRK applied to the unfolded tensor system

$$\text{bcirc}(\mathcal{A}) \text{ unfold}(\mathcal{X}) = \text{unfold}(\mathcal{B}).$$

These experiments demonstrate the computational benefits of using TRK given by Equation (6) over applying standard MRK to an unfolded system.

### 6.1 Contraction coefficients of TRK and MRK

In this experiment, the contraction coefficient of the proposed TRK is compared to that of MRK. In order to apply the standard MRK method to recover the three-dimensional signal  $\mathcal{X}$ , we unfold the tensor  $\mathcal{X}$  into the matrix unfold  $(\mathcal{X}) \in \mathbb{C}^{\ell n \times p}$  and collect measurements  $\mathbf{B} \in \mathbb{C}^{\mu \times p}$  of the signal  $\mathcal{X}$  via the measurement matrix  $\mathbf{A} \in \mathbb{C}^{\mu \times n\ell}$ , resulting in the matrix linear system

$$\mathbf{A} \text{unfold}(\mathcal{X}) = \mathbf{B}. \quad (24)$$

After each iteration of MRK applied to Equation (24), the iterate unfold  $(\mathcal{X}^{t+1})$  satisfies

$$\mathbf{A}_{i_t:} \text{unfold}(\mathcal{X}^{t+1}) = \text{unfold}(\mathbf{B})_{i_t:}. \quad (25)$$

Thus, the constraint is applied to each column of  $\text{unfold}(\mathcal{X})$  or equivalently each column slice of  $\mathcal{X}$  independently. Note that the measurement matrix  $\mathbf{A}$  will have the same number of elements as the measurement tensor  $\mathcal{A}$  in Equation (3) if  $\mu = m$ .

Assuming that the rows of  $\mathbf{A}$  are normalized, MRK applied to matrix linear systems has a contraction coefficient of

$$1 - \sigma_{\min}^2(\mathbf{A})/m. \quad (26)$$

For TRK, the contraction coefficient from Theorem 11 is

$$1 - \min_{k \in [n-1]} \frac{\sigma_{\min}^2(\hat{\mathcal{A}}_k)}{m \left\| \hat{\mathcal{A}}_k \right\|_{\infty,2}^2}.$$

In this experiment, row slices  $\mathcal{A}_{i:}$  have unit Frobenius norm and indices  $i \in [m-1]$  are selected uniformly at random at each iteration.

The measurement matrix  $\mathbf{A} \in \mathbb{C}^{m \times \ell n}$  and measurement tensor  $\mathcal{A} \in \mathbb{C}^{m \times \ell \times n}$  are generated as follows. The entries of  $\mathbf{A} \in \mathbb{C}^{m \times \ell n}$  are drawn i.i.d. from a standard Gaussian distribution and then each row is normalized to have unit norm. The entries of  $\mathcal{A} \in \mathbb{R}^{m \times \ell \times n}$  are also drawn i.i.d. from a standard Gaussian distribution but row slices  $\mathcal{A}_{i:}$  (as opposed to matrix rows) of  $\mathcal{A}$  are normalized to have unit Frobenius norm. Note that both the tensor  $\mathcal{A}$  and matrix  $\mathbf{A}$  in this experiment have the same memory complexity of  $\mathcal{O}(m\ell n)$ . The contraction coefficients, computed via Equation (26) for matrices  $\mathbf{A}$  and Equation (16) for tensors  $\mathcal{A}$ , with a varying number of measurements  $m$  are presented in Figure 2. Here, the dimensions  $\ell = 20$  and  $n = 10$  are fixed. For each number of measurements  $m$ , the contraction coefficients are averaged over 50 random realizations of the measurement tensor or matrix.

In this experiment, the contraction coefficients for MRK and TRK differ, with TRK being smaller (i.e., faster convergence) for larger  $m$ . Thus, in the

large-scale setting where  $m \gg \ell n$ , TRK is expected to converge faster than MRK, as we will see in the experiments of Section 6.2. When a small number of measurements  $m$  are used, MRK has a smaller contraction coefficient than TRK, however, we are primarily concerned with the setting in which  $m \gg \ell n$  as this is the typical use case for Kaczmarz methods.

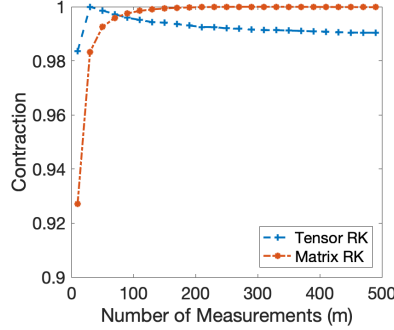


Figure 2: Comparison between contraction coefficients of MRK (Equation (26)) applied to a matrix linear system and TRK (Equation (16)) applied to a tensor system.

## 6.2 Empirical performance of TRK and MRK

We now compare the empirical performance of MRK and TRK on linear systems  $\mathcal{A}\mathcal{X} = \mathcal{B}$  and  $\mathbf{A}\mathbf{X} = \mathbf{Y}$ . Similar to the previous experiment, the dimensions of  $\mathcal{A}$  and  $\mathbf{A}$  are selected to require a similar measurement complexity while solving for unknown signals of comparable dimensions. More specifically, for the tensor system we have  $\mathcal{A} \in \mathbb{C}^{m \times \ell \times n}$  and  $\mathcal{X} \in \mathbb{C}^{\ell \times p \times n}$ , while for the matrix system, we have  $\mathbf{A} \in \mathbb{C}^{m \times \ell n}$  and  $\mathbf{X} \in \mathbb{C}^{\ell n \times p}$ . The entries of  $\mathcal{A}$  and  $\mathbf{A}$  are initialized with i.i.d. standard Gaussian entries then normalized to have unit row slice and matrix row Frobenius norm respectively. The entries of the signals  $\mathcal{X}$  and  $\mathbf{X}$  are drawn i.i.d. from a standard Gaussian distribution and the empirical results presented here are averaged over 20 random runs of TRK and MRK. For TRK, we use the implementation outlined in Algorithm 2.

Figure 3 compares the empirical performances of the two algorithms for an over-determined system with  $m = 500$ ,  $\ell = 20$ ,  $n = 10$ , and  $p = 10$ . We refer to a tensor linear system as over-determined if the Fourier transformed systems of Equation (18) is over-determined, i.e., if  $m \geq \ell$ . In the over-determined setting, we plot the convergence of the algorithms with respect to iterations (left plot) as well as CPU time (right plot). We observe that in both settings, TRK outperforms MRK in terms of iterations and CPU times. While, visually, MRK does not seem to be making progress towards the solution in either setting, it is in fact converging slowly. This should not be surprising given the equivalence between TRK and block MRK. In particular, one can think of TRK as block

MRK acting on  $n$  rows at a time (whereas MRK only works on one row at a time).

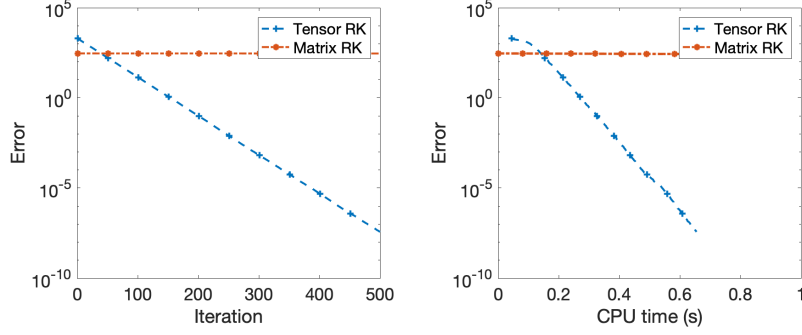


Figure 3: Comparison MRK and TRK when the measurement matrix (or tensor) has a fixed memory budget of  $\mathcal{O}(mln)$  bits when  $m = 500$ ,  $\ell = 20$ , and  $n = 10$ .

We additionally consider the setting in which one is immediately provided the measurement tensor  $\mathcal{A} \in \mathbb{C}^{m \times \ell \times n}$  and corresponding measurements  $\mathcal{B} \in \mathbb{C}^{m \times p \times n}$  and can choose between performing signal recovery using TRK or by unfolding the tensor system and solving  $\text{bcirc}(\mathcal{A}) \text{unfold}(\mathcal{X}) = \text{unfold}(\mathcal{B})$  using MRK.

The tensor  $\mathcal{A}$  is initialized with i.i.d. standard Gaussian entries and the measurement matrix  $\mathbf{A}$  is taken to be  $\mathbf{A} = \text{bcirc}(\mathcal{A})$ . Here,  $m = 100$ ,  $\ell = 15$ ,  $n = 10$ , and  $p = 30$ . Figure 4 plots the resulting empirical performance averaged over 20 random runs of TRK and MRK when choosing between signal recovery using TRK or MRK for a given tensor measurement system. We again see that TRK converges at a much faster rate than MRK in this setting.

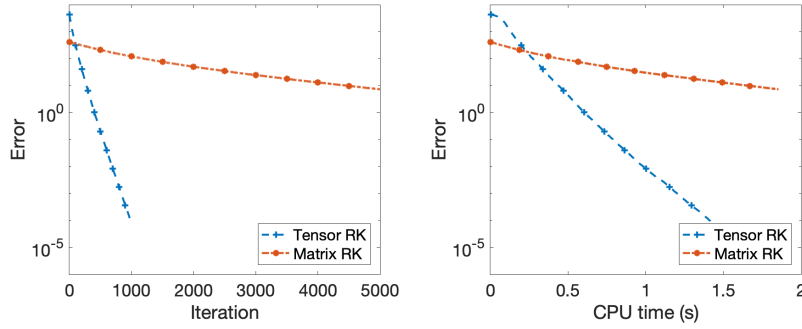


Figure 4: Performance comparison of MRK on matricized linear system and TRK on tensor linear system.

### 6.3 Empirical performance of TRK and block MRK

To support the theoretical guarantees and remarks regarding the equivalence of TRK and block MRK, experimental results comparing the empirical performance of the two algorithms are presented in this section. In Figure 5, TRK and block MRK are used to solve a tensor linear system as shown in Equation (3). TRK solves the tensor system via the update in Equation (6) while block MRK is performed on the transformed system in the Fourier domain given in Equation (18) with predetermined blocks  $\tau_i = \{km+i \mid k \in [n-1]\}$ . The measurement tensor  $\mathcal{A} \in \mathbb{R}^{100 \times 30 \times 5}$  and signal tensor  $\mathcal{X} \in \mathbb{R}^{30 \times 15 \times 5}$  contains i.i.d. standard Gaussian entries. All approximation errors are averaged over 20 runs of the respective algorithm. The theoretical upper bounds, titled in the legend with ‘UB’, are computed using Equation (17) for TRK and Equation (23) for block MRK. Figure 5 clearly shows that TRK and block MRK perform similarly across iterations as expected since the two methods are shown to be equivalent in Section 5.3. As remarked, the TRK upper bound shown in Theorem 11 has a slight advantage over the general block MRK convergence guarantees as these do not make use of the block diagonal structure of Equation (18). Experiments comparing CPU times for TRK and block MRK are omitted, as the two methods are equivalent as shown in Section 5.3 and highly optimized algorithms exist for the matrix implementation.

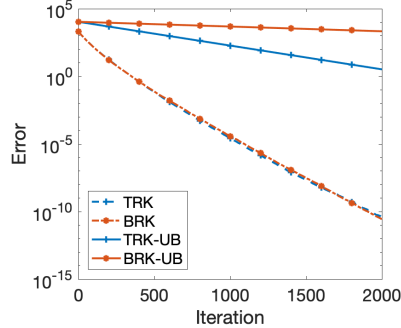


Figure 5: Performance of TRK and block MRK on a tensor linear system. ‘TRK-UB’ and ‘BRK-UB’ indicate the theoretical upper bounds of TRK and block MRK respectively.

## 7 Conclusion

This work extends the randomized Kaczmarz literature to solve large-scale tensor linear systems under the t-product. The proposed tensor randomized Kaczmarz (TRK) algorithm solves large-scale tensor linear systems and is guaranteed to converge exponentially in expectation. Connections to the block randomized Kaczmarz are made and empirical results are provided to support derived



theoretical guarantees. This work further provides a framework to extend other stochastic iterative methods that arise in literature such as the randomized extended Kaczmarz algorithm, randomized Gauss-Seidel algorithm, coordinate descent, sketch-and-project [9], and many more.

## Acknowledgements

This work began at the 2019 workshop for Women in Science of Data and Math (WISDM) held at the Institute for Computational and Experimental Research in Mathematics (ICERM). This workshop is partially supported by an NSF ADVANCE grant (award #1500481) to the Association for Women in Mathematics (AWM). Ma was partially supported by U.S. Air Force Award FA9550-18-1-0031 led by Roman Vershynin. Molitor is grateful to and was partially supported by NSF CAREER DMS #1348721 and NSF BIGDATA DMS #1740325 led by Deanna Needell. The authors would also like to thank Misha Kilmer for her advising during the WISDM workshop and valuable feedback that improved earlier versions of this manuscript.

## A Proofs for properties of block circulant matrices

We use properties of circulant matrices and the Kronecker product in proving Facts 1 and 2. For a vector  $v \in \mathbb{C}^n$

$$\text{circ}(v) = \begin{pmatrix} v_0 & v_{n-1} & \dots & v_1 \\ v_1 & v_0 & \dots & v_2 \\ \vdots & \vdots & \ddots & \vdots \\ v_{n-2} & v_{n-3} & \dots & v_{n-1} \\ v_{n-1} & v_{n-2} & \dots & v_0 \end{pmatrix}.$$

The block circulant of a matrix  $\text{bcirc}(\mathcal{M})$  can be decomposed as

$$\text{bcirc}(\mathcal{M}) = \sum_{i=0}^{n-1} \text{circ}(e_i) \otimes \mathcal{M}_{::i}, \quad (27)$$

where  $e_i$  is the  $i^{\text{th}}$  standard basis vector in  $\mathbb{C}^n$  and  $\otimes$  denotes the Kronecker product.

### A.1 Proof of Fact 1

Recall that Fact 1 states

$$\text{bcirc}(\mathcal{AB}) = \text{bcirc}(\mathcal{A}) \text{bcirc}(\mathcal{B}).$$

*Proof.* Decomposing  $\text{bcirc}(\mathcal{AB})$ , Equation (27) obtains the equality

$$\text{bcirc}(\mathcal{AB}) = \sum_{i=0}^{n-1} \text{circ}(e_i) \otimes (\mathcal{AB})_{::i}.$$

For notational simplicity, let  $\mathbf{A}_i = \mathcal{A}_{::i}$  and  $\mathbf{B}_i = \mathcal{B}_{::i}$  denote the  $i^{\text{th}}$  frontal faces of  $\mathcal{A}$  and  $\mathcal{B}$  respectively. Then

$$\begin{aligned} (\mathcal{AB})_{::i} &= \text{fold}(\text{bcirc}(\mathcal{A}) \text{unfold}(\mathcal{B}))_{::i} \\ &= (\mathbf{A}_i \quad \mathbf{A}_{i-1} \quad \dots \quad \mathbf{A}_0 \quad \mathbf{A}_{n-1} \quad \dots \quad \mathbf{A}_{i+1}) \text{unfold}(\mathcal{B}) \\ &= \mathbf{A}_i \mathbf{B}_0 + \mathbf{A}_{i-1} \mathbf{B}_1 + \dots + \mathbf{A}_0 \mathbf{B}_i + \mathbf{A}_{n-1} \mathbf{B}_{i+1} + \dots + \mathbf{A}_{i+1} \mathbf{B}_{n-1} \\ &= \sum_{k=0}^{n-1} \mathbf{A}_{i-k \pmod{n}} \mathbf{B}_k. \end{aligned}$$

We then have that

$$\text{bcirc}(\mathcal{AB}) = \sum_{i=0}^{n-1} \sum_{k=0}^{n-1} \text{circ}(e_i) \otimes \mathbf{A}_{i-k \pmod{n}} \mathbf{B}_k.$$

Changing  $i \rightarrow i+k$ , we can rewrite this as

$$\text{bcirc}(\mathcal{AB}) = \sum_{i=0}^{n-1} \sum_{k=0}^{n-1} \text{circ}(e_{i+k \pmod{n}}) \otimes \mathbf{A}_i \mathbf{B}_k. \quad (28)$$

Similarly, we can decompose  $\text{bcirc}(\mathcal{A}) \text{bcirc}(\mathcal{B})$  as

$$\begin{aligned} \text{bcirc}(\mathcal{A}) \text{bcirc}(\mathcal{B}) &= \left( \sum_{i=0}^{n-1} \text{circ}(e_i) \otimes \mathbf{A}_i \right) \left( \sum_{k=0}^{n-1} \text{circ}(e_k) \otimes \mathbf{B}_k \right) \\ &= \sum_{i=0}^{n-1} \sum_{k=0}^{n-1} (\text{circ}(e_i) \otimes \mathbf{A}_i) (\text{circ}(e_k) \otimes \mathbf{B}_k). \end{aligned}$$

The mixed-product property further gives

$$\begin{aligned} \text{bcirc}(\mathcal{A}) \text{bcirc}(\mathcal{B}) &= \sum_{i=0}^{n-1} \sum_{k=0}^{n-1} \text{circ}(e_i) \text{circ}(e_k) \otimes \mathbf{A}_i \mathbf{B}_k \\ &= \sum_{i=0}^{n-1} \sum_{k=0}^{n-1} \text{circ}(e_{i+k \pmod{n}}) \otimes \mathbf{A}_i \mathbf{B}_k. \end{aligned}$$

We have now recovered the right-hand side of Equation (28) and thus  $\text{bcirc}(\mathcal{AB}) = \text{bcirc}(\mathcal{A}) \text{bcirc}(\mathcal{B})$  as desired.  $\square$

## A.2 Proof of Fact 2

Fact 2 states

$$\text{bcirc}(\mathcal{M}^*) = \text{bcirc}(\mathcal{M})^*.$$

*Proof.* For simplicity, let  $\mathbf{M}_i = \mathcal{M}_{::i}$  denote the  $i^{\text{th}}$  frontal face of  $\mathcal{M}$ . Decomposing  $\text{bcirc}(\mathcal{M})$  as in Equation (27), using the definition of the tensor transpose, the fact that  $(\mathbf{A} \otimes \mathbf{B})^* = \mathbf{A}^* \otimes \mathbf{B}^*$  and  $\text{circ}(e_i)^* = \text{circ}(e_{n-i})$  [19],

$$\begin{aligned} \text{bcirc}(\mathcal{M}^*) &\stackrel{(27)}{=} \sum_{i=0}^{n-1} \text{circ}(e_i) \otimes (\mathcal{M}^*)_{::i} \\ &= \mathbf{I}_n \otimes (\mathbf{M}_1)^* + \sum_{i=1}^{n-1} \text{circ}(e_i) \otimes (\mathbf{M}_{n-i})^* \\ &= \mathbf{I}_n^* \otimes (\mathbf{M}_1)^* + \sum_{i=1}^{n-1} \text{circ}(e_{n-i})^* \otimes (\mathbf{M}_{n-i})^* \\ &= \left[ \mathbf{I}_n \otimes (\mathbf{M}_1) + \sum_{i=1}^{n-1} \text{circ}(e_{n-i}) \otimes (\mathbf{M}_{n-i}) \right]^* \\ &= \text{bcirc}(\mathcal{M})^*. \end{aligned}$$

□

## B Tensor Pythagorean Theorem

An analogue of the Pythagorean Theorem is stated and proved for tensors.

**Lemma 12.** *For an orthogonal projection  $\mathcal{P}$  and tensor  $\mathcal{M}$  of compatible size,*

$$\|\mathcal{M}\|_F^2 = \|(\mathcal{I} - \mathcal{P})\mathcal{M}\|_F^2 + \|\mathcal{P}\mathcal{M}\|_F^2.$$

*Proof.* This result can be shown by rewriting the tensor products in terms of matrix products and applying Lemma 4. Note that for a tensor  $\mathcal{M}$ ,

$$\|\mathcal{M}\|_F^2 = \|\text{unfold}(\mathcal{M})\|_F^2.$$

Decomposing  $\|\mathcal{M}\|_F^2$  and rewriting the result in terms of matrices,

$$\begin{aligned} \|\mathcal{M}\|_F^2 &= \|(\mathcal{I} - \mathcal{P})\mathcal{M} + \mathcal{P}\mathcal{M}\|_F^2 \\ &= \|\text{bcirc}(\mathcal{I} - \mathcal{P})\text{unfold}(\mathcal{M}) + \text{bcirc}(\mathcal{P})\text{unfold}(\mathcal{M})\|_F^2. \end{aligned}$$

Since  $\text{bcirc}(\mathcal{P})$  is an orthogonal projection (Lemma 4), by the Pythagorean theorem,

$$\begin{aligned} \|\mathcal{M}\|_F^2 &= \|\text{bcirc}(\mathcal{I} - \mathcal{P})\text{unfold}(\mathcal{M})\|_F^2 + \|\text{bcirc}(\mathcal{P})\text{unfold}(\mathcal{M})\|_F^2 \\ &= \|(\mathcal{I} - \mathcal{P})\mathcal{M}\|_F^2 + \|\mathcal{P}\mathcal{M}\|_F^2. \end{aligned}$$

□

## References

- [1] S. Agmon. The relaxation method for linear inequalities. *Canadian J. Math.*, 6:382–392, 1954.
- [2] A. Anandkumar, R. Ge, and M. Janzamin. Learning overcomplete latent variable models through tensor methods. In *COLT*, pages 36–112, 2015.
- [3] B. W. Bader and T. G. Kolda. Algorithm 862: MATLAB tensor classes for fast algorithm prototyping. *ACM T. Math. Software*, 32(4):635–653, 2006.
- [4] Y. Censor. Row-action methods for huge and sparse systems and their applications. *SIAM Rev.*, 23(4):444–466, 1981.
- [5] L. De Lathauwer, B. De Moor, and J. Vandewalle. A multilinear singular value decomposition. *SIAM J. Matrix Anal. A.*, 21(4):1253–1278, 2000.
- [6] J. A. De Loera, J. Haddock, and D. Needell. A sampling Kaczmarz–Motzkin algorithm for linear feasibility. *SIAM J. Sci. Comput.*, 39(5):S66–S87, 2017.
- [7] P. Drineas and M. W. Mahoney. Randnla: randomized numerical linear algebra. *Commun. ACM*, 59(6):80–90, 2016.
- [8] T. Elfving. Block-iterative methods for consistent and inconsistent linear equations. *Numer. Math.*, 35(1):1–12, 1980.
- [9] R. M. Gower and P. Richtárik. Randomized iterative methods for linear systems. *SIAM J. Matrix Anal. A.*, 36(4):1660–1690, 2015.
- [10] J. Haddock and D. Needell. On Motzkin’s method for inconsistent linear systems. *BIT*, 59(2):387–401, 2019.
- [11] N. Hao, M. E. Kilmer, K. Braman, and R. C. Hoover. Facial recognition using tensor-tensor decompositions. *SIAM J. Imaging Sci.*, 6(1):437–463, 2013.
- [12] G.-B. Huang, L. Chen, C. K. Siew, et al. Universal approximation using incremental constructive feedforward networks with random hidden nodes. *IEEE T. Neural Networ.*, 17(4):879–892, 2006.
- [13] M. S. Kaczmarz. Angenäherte auflösung von systemen linearer gleichungen. *Bull. Acad. Polonaise Sci. Lett.*, 35:355–357, 1937.
- [14] E. Kernfeld, M. Kilmer, and S. Aeron. Tensor–tensor products with invertible linear transforms. *Linear Algebra App.*, 485:545–570, 2015.
- [15] H. A. Kiers. Towards a standardized notation and terminology in multiway analysis. *J. Chemometr.*, 14(3):105–122, 2000.
- [16] M. E. Kilmer, K. Braman, N. Hao, and R. C. Hoover. Third-order tensors as operators on matrices: A theoretical and computational framework with applications in imaging. *SIAM J. Matrix Anal. A.*, 34(1):148–172, 2013.

- [17] M. E. Kilmer and C. D. Martin. Factorization strategies for third-order tensors. *Linear Algebra App.*, 435(3):641–658, 2011.
- [18] Y. Koren, R. Bell, and C. Volinsky. Matrix factorization techniques for recommender systems. *Computer*, 42(8):30–37, 2009.
- [19] I. Kra and S. R. Simanca. On circulant matrices. *Not. Am. Math. Soc.*, 59(3):368–377, 2012.
- [20] Z. Liu, H. V. Zhao, and A. Y. Elezzabi. Block-based adaptive compressed sensing for video. In *IEEE Image Proc.*, pages 1649–1652. IEEE, 2010.
- [21] A. Ma, D. Needell, and A. Ramdas. Convergence properties of the randomized extended Gauss–Seidel and Kaczmarz methods. *SIAM J. Matrix Anal. A.*, 36(4):1590–1604, 2015.
- [22] A. Majumdar and R. K. Ward. Face recognition from video: An MMV recovery approach. In *Int. Conf. Acoust. Spee.*, pages 2221–2224. IEEE, 2012.
- [23] T. S. Motzkin and I. J. Schoenberg. The relaxation method for linear inequalities. *Canadian J. Math.*, 6:393–404, 1954.
- [24] D. Needell. Randomized Kaczmarz solver for noisy linear systems. *BIT*, 50(2):395–403, 2010.
- [25] D. Needell and J. A. Tropp. Paved with good intentions: analysis of a randomized block Kaczmarz method. *Linear Algebra App.*, 441:199–221, 2014.
- [26] D. Needell, R. Ward, and N. Srebro. Stochastic gradient descent, weighted sampling, and the randomized Kaczmarz algorithm. In *Adv. Neur. In.*, pages 1017–1025, 2014.
- [27] E. Newman, L. Horesh, H. Avron, and M. Kilmer. Stable tensor neural networks for rapid deep learning. *arXiv preprint arXiv:1811.06569*, 2018.
- [28] E. Newman and M. E. Kilmer. Non-negative Tensor Patch Dictionary Approaches for Image Compression and Deblurring Applications. *arXiv e-prints*, page arXiv:1910.00993, Sep 2019.
- [29] J. Nutini, B. Sepehry, A. Virani, I. Laradji, M. Schmidt, and H. Koepke. Convergence rates for greedy Kaczmarz algorithms. In *UAI*, 2016.
- [30] S. Petra and C. Popa. Single projection Kaczmarz extended algorithms. *Numer. Algorithms*, 73(3):791–806, 2016.
- [31] F. Roemer, G. Del Galdo, and M. Haardt. Tensor-based algorithms for learning multidimensional separable dictionaries. In *Int. Conf. Acoust. Spee.*, pages 3963–3967, 2014.

- [32] O. Semerci, N. Hao, M. E. Kilmer, and E. L. Miller. Tensor-based formulation and nuclear norm regularization for multienergy computed tomography. *IEEE T. Image Proces.*, 23(4):1678–1693, 2014.
- [33] S. Soltani, M. E. Kilmer, and P. C. Hansen. A tensor-based dictionary learning approach to tomographic image reconstruction. *BIT*, 56(4):1425–1454, 2016.
- [34] T. Strohmer and R. Vershynin. A randomized Kaczmarz algorithm with exponential convergence. *J. Fourier Anal. Apps.*, 15(2):262, 2009.
- [35] S. Tan, Y. Zhang, G. Wang, X. Mou, G. Cao, Z. Wu, and H. Yu. Tensor-based dictionary learning for dynamic tomographic reconstruction. *Phys. Med. Biol.*, 60(7):2803, 2015.
- [36] X. Wang, M. Che, and Y. Wei. Tensor neural network models for tensor singular value decompositions. *Comput. Optim. Appl.*, 75(3):753–777, 2020.
- [37] Y. Zhang, X. Mou, G. Wang, and H. Yu. Tensor-based dictionary learning for spectral CT reconstruction. *IEEE T. Med. Imaging*, 36(1):142–154, 2017.
- [38] Z. Zhang and S. Aeron. Denoising and completion of 3d data via multidimensional dictionary learning. In *Int. Join. Conf. Artif.*, pages 2371–2377, 2016.
- [39] Z. Zhang and S. Aeron. Exact tensor completion using t-SVD. *IEEE T. Signal Proces.*, 65(6):1511–1526, 2017.
- [40] Z. Zhang, G. Ely, S. Aeron, N. Hao, and M. Kilmer. Novel methods for multilinear data completion and de-noising based on tensor-SVD. In *CVPR*, pages 3842–3849. IEEE, 2014.
- [41] P. Zhou, C. Lu, Z. Lin, and C. Zhang. Tensor factorization for low-rank tensor completion. *IEEE T. Image Proces.*, 27(3):1152–1163, 2018.
- [42] A. Zouzias and N. M. Freris. Randomized extended Kaczmarz for solving least squares. *SIAM J. Matrix Anal. Appl.*, 34(2):773–793, 2013.
- [43] S. Zubair and Wenwu Wang. Tensor dictionary learning with sparse tucker decomposition. In *Int. Conf. Digit. Sig.*, pages 1–6, 2013.